Leading nucleon production at HERA and the structure of the pion

Garry Levman

Department of Physics, University of Toronto, 60 St George St, Toronto ON M5S 1A7, Canada

E-mail: levman@physics.utoronto.ca

Abstract.

Experimental results from HERA on the production of leading neutrons in neutral current e^+p collisions are reviewed. The data cover a large kinematic range from photoproduction to deep inelastic scattering. The neutrons are produced with low transverse momentum ($p_T < 0.7$ GeV) and carry a large fraction of the incoming proton's energy ($x_L > 0.2$). Neutron production is studied relative to the inclusive cross section, reducing considerably the systematic error. The rate of neutrons in photoproduction is about half that expected from hadroproduction experiments. The photoproduction and hadroproduction data are otherwise in agreement and broadly in accord with particle-exchange models. There is a 20-30% rise in the rate of neutrons between photoproduction and deep inelastic scattering attributable to absorptive rescattering in the γ^*p system. Aside from absorptive effects, the rate of neutron production depends only logarithmically on Q^2, the virtuality of the exchanged photon, and x, the momentum fraction of the incoming proton carried by the struck quark. Factorization breaking is observed: for $0.64 < x_L < 0.82$ the rate of neutrons is almost independent of the leptonic variables; however, at low and high x_L there is a weak dependence. Over the whole kinematic range from photoproduction to deep inelastic scattering, the structure function for leading neutron production is approximately given by $F_2^{LN(3)}(x, Q^2, x_L) = A(Q^2)F_2(x, Q^2)f(x_L)$, where F_2 is the structure function of the proton, $f(x_L)$ is the flux of neutrons, and $A(Q^2)$ is an absorptive factor. The total $\gamma\pi$ cross section in photoproduction, $\sigma(\gamma\pi)$, and the structure function of pion in deep inelastic scattering, F_2^π, can be extracted from the data on the assumption that pion exchange is the dominant mechanism for the production of leading neutrons. An effective flux method is introduced which avoids many theoretical uncertainties. $\sigma(\gamma\pi)$ is found to be approximately one-third $\sigma(\gamma p)$, violating quark counting rules which predict two-thirds. The x and Q^2 dependence of F_2^π is similar to F_2.

1. Introduction

The confinement of partons, the nature of the vacuum, and the long range structure of hadrons remain puzzles of quantum chromodynamics closely related to the problem of the transition from perturbative to non-perturbative physics.

Leading nucleons have been observed in positron-proton collisions at HERA [1–3]. These are protons and neutrons which carry a large fraction of the energy ($x_L \gtrsim 0.2$) of the target proton, but which are produced with small transverse momentum ($p_T \lesssim 0.7$ GeV). The presence of a leading nucleon in the final state flags a peripheral process associated with long distances, even when short distances are probed by high photon virtuality (Q^2) or high transverse energies. The study of leading nucleon production therefore provides information on the relationship between the soft and hard aspects of the strong interaction.

Only the structure of the nucleon is directly accessible to experimental study in leptoproduction experiments. As a result, in comparison to the nucleon, mesons are poorly understood. Meson exchange theory has been successful at describing leading nucleon production in hadroproduction. Applied to leptoproduction experiments, it can be used to obtain information about meson-photon cross sections and about the partonic structure of mesons. The structure of the pion is particularly interesting: it is a Goldstone boson of the strong interaction [4], and it is conjectured to play an important role in color confinement [5–7]. Because pion exchange is expected to dominate leading neutron production [8–10], it is pion structure that is mainly probed in neutron tagged leptoproduction experiments.

The theory for leading proton production is more complicated than for neutrons. There is a large diffractive component absent in the case of leading neutrons. Isoscalar mesons such as the f and ω also contribute. In addition, isospin factors reduce the contribution of pion exchange for direct production $p \to p$, but enhance pion exchange for indirect production [11] $p \to \Delta \to p$. This paper concentrates on the leading neutron data although attention will be paid to leading protons.

The data from HERA cover a large kinematic range: from photoproduction $Q^2 < 0.02$ GeV^2, through a transition region $0.1 < Q^2 < 0.8$ GeV^2, to deep inelastic scattering (DIS) $Q^2 > 4$ GeV^2. The studies include both semi-inclusive reactions [1, 2, 12, 13], $ep \to enX$, as well as the semi-exclusive production of jets with high transverse energy [3, 14], $ep \to en\ jet\ jet\ X$.

In analogy with the inclusive structure function $F_2(x, Q^2)$, which is defined by the two-fold inclusive ep cross section,

$$\frac{d^2\sigma(ep \to eX)}{dxdQ^2} = \frac{4\pi\alpha^2}{dxQ^4}\left(1 - y + \frac{y^2}{2}\right) F_2(x, Q^2)$$

the semi-inclusive structure function $F_2^{LB(4)}(x, Q^2, x_L, p_T^2)$ is defined by the four-fold differential cross section for leading baryon production,

$$\frac{d^4\sigma(ep \to eBX)}{dxdQ^2dx_Ldp_T^2} = \frac{4\pi\alpha^2}{xQ^4}\left(1 - y + \frac{y^2}{2}\right) F_2^{LB(4)}(x, Q^2, x_L, p_T^2)$$

where $B = (p, n)$; x is Bjorken's variable, the fraction of the incoming proton's momentum carried by the struck quark; and y is the inelasticity of the electron in the rest frame of the target proton. Integration of the cross section equation over p_T gives the structure function $F_2^{LB(3)}(x, Q^2, x_L)$.

The rate of leading neutron production relative to the inclusive cross section is given by the ratio of the semi-inclusive to the inclusive cross section. Because of the cancellation of kinematic factors this ratio is F_2^{LB}/F_2. The correction factors for radiation, Z exchange, and the longitudinal structure function F_L may be neglected since they depend only on the *difference* between the corrections for the inclusive and semi-inclusive cases. The study of ratios reduces considerably both the theoretical and systematic uncertainties.

The data discussed below were taken at HERA between 1995 and 1997 with 27.5 GeV positrons colliding with 820 GeV protons.

2. Leading proton production

The leading protons display many characteristics similar to leading neutron production. The open circles in Fig. 1 show the H1 measurement [2] of F_2^{LP} for protons in the kinematical range $2 < Q^2 < 50$ GeV^2, $0.7 < x_L < 0.9$ and $p_T < 0.2$ GeV. In each bin of x and Q^2 the structure function is approximately flat in x_L; however, the values increase with increasing Q^2. The flatness of the x_L distribution for protons is also apparent in the ZEUS data [12], presented in Fig. 2, which show that there is no difference in shape or rate between DIS and the transition region ($0.1 < Q^2 < 0.8$ GeV^2). ZEUS has also studied the angular distribution of leading protons as a function of x_L in the transition region and in DIS. In bins of x_L the data are well described by $dN/dp_T^2 \propto \exp(-bp_T^2)$. The values found for the slope parameters b are largely independent of x_L, and are the same in both the DIS and the transition samples (Fig. 3).

The proton rate approximately doubles between $Q^2 \approx 0$ and $Q^2 \approx 10$ GeV^2 in DIS as seen in Fig. 4 which shows that the rise is independent of x_L and W, the invariant mass of the hadronic system recoiling off the incoming positron. For DIS alone, the rate of leading protons is independent of the kinematic variables of the lepton (not shown).

In summary, approximately 15% of the DIS events have a leading proton with $0.6 < x_L < 0.9$ and $p_T^2 < 0.5$ GeV^2, but only half that many for photoproduction. The data indicate that

$$F_2^{LP}(x, Q^2, x_L, p_T^2) \propto A(Q^2) \exp(-6p_T^2) F_2(x, Q^2)$$

with p_T in GeV. $A(Q^2)$ is a factor to account for the absorption of protons at low Q^2. The positron variables x and Q^2 factorize from the proton variables x_L and p_T, a form of the hypothesis of limiting fragmentation [15].

3. Leading neutron production

The filled circles in Fig. 1 show the H1 measurement of F_2^{LN} at high x_L. In contrast to the leading proton case, F_2^{LN} decreases with increasing x_L approaching zero at the kinematic limit.

ZEUS has measured the x_L spectrum of neutrons in photoproduction ($Q^2 < 0.02$ GeV^2) the transition region ($0.1 < Q^2 < 0.74$ GeV^2) and DIS ($Q^2 > 4$ GeV^2). The data are shown in Fig. 5 as a fraction of the corresponding total inclusive cross section. The

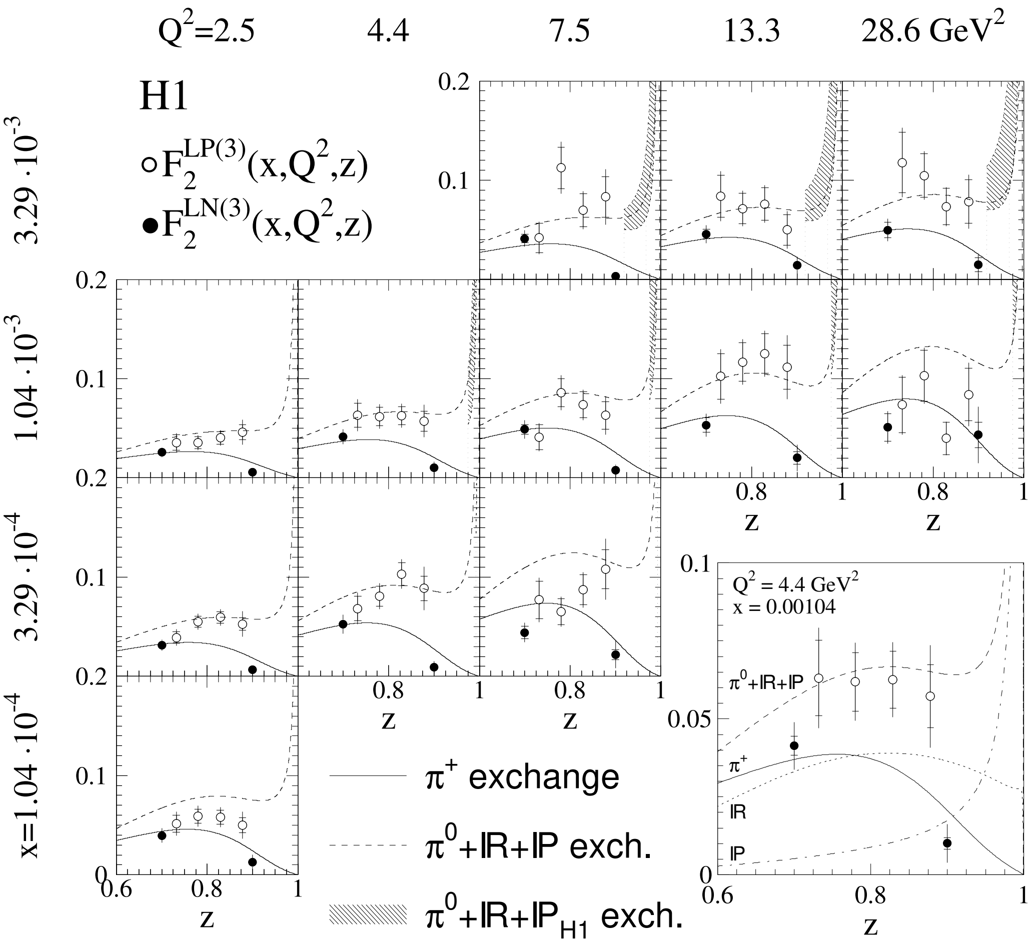

Figure 1. F_2^{LP} and F_2^{LN} as a function of $z \equiv x_L$ in bins of x and Q^2. The structure functions are integrated over $0 < p_T < 0.2$ GeV. The curves show the result of the H1 particle-exchange model for leading nucleon production. The amount of pion exchange in nucleon production is fixed by neutron production. $I\!R$ represents the remaining meson exchanges contributing to proton production. $I\!P$ is the diffractive component (pomeron exchange).

neutron production angles are restricted to $\theta < 0.8$ mrad by the proton beam line, so that $p_T < 0.66x_L$ GeV. The increase in the p_T range with x_L accounts for much of the rising neutron yield with x_L.

The neutron rate increases by 20-30% between photoproduction and DIS. For DIS the spectra are roughly independent of Q^2, although at low x_L the rate continues to increase slowly while at high x_L the rate decreases as seen in Fig. 6. In the peak region, $0.64 < x_L < 0.82$, the neutron yield in DIS is approximately independent of x and Q^2.

ZEUS has also measured the angular distribution of neutrons in DIS. In contrast

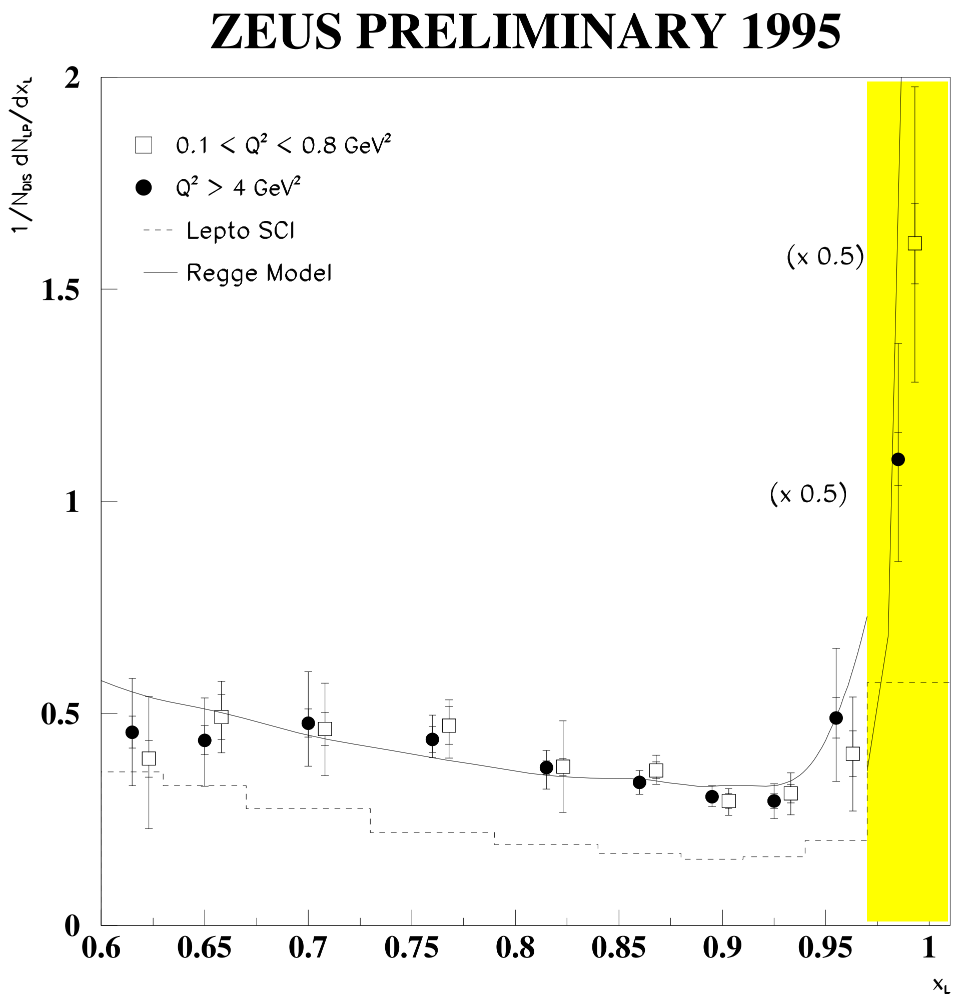

Figure 2. The rate of proton production ($p_T^2 < 0.5^2$ GeV^2) for DIS ($Q^2 > 4$ GeV^2) and for the transition region ($0.1 < Q^2 < 0.8$ GeV^2) as a function of x_L. The diffractive peak is seen at $x_L \gtrsim 0.95$. The solid curve shows the expectation of a particle exchange model [37]. The histogram shows the expectation of the LEPTO Monte Carlo program [38] with soft color interactions [39].

to the case of leading protons, the b slopes for neutron production rise rapidly with increasing x_L as seen in Fig. 7.

In summary, approximately 7.5% of the events in DIS have a leading neutron with $0.2 < x_L < 1$ and $p_T < 0.66x_L$ GeV. The data indicate that $F_2^{LN(3)}(x, Q^2, x_L) \propto A(Q^2)F_2(x, Q^2)f(x_L)$, where F_2 is the structure function of the proton, $f(x_L)$ is the flux of neutrons, and $A(Q^2)$ is an absorptive factor.

4. Absorption

HERA is unique in providing the experimenter with a projectile whose size can be varied. At $Q^2 = 0$ the photon has a size which is typical of a hadron (rho dominance). As Q^2 increases the photon's size decreases with the consequence that absorptive rescattering

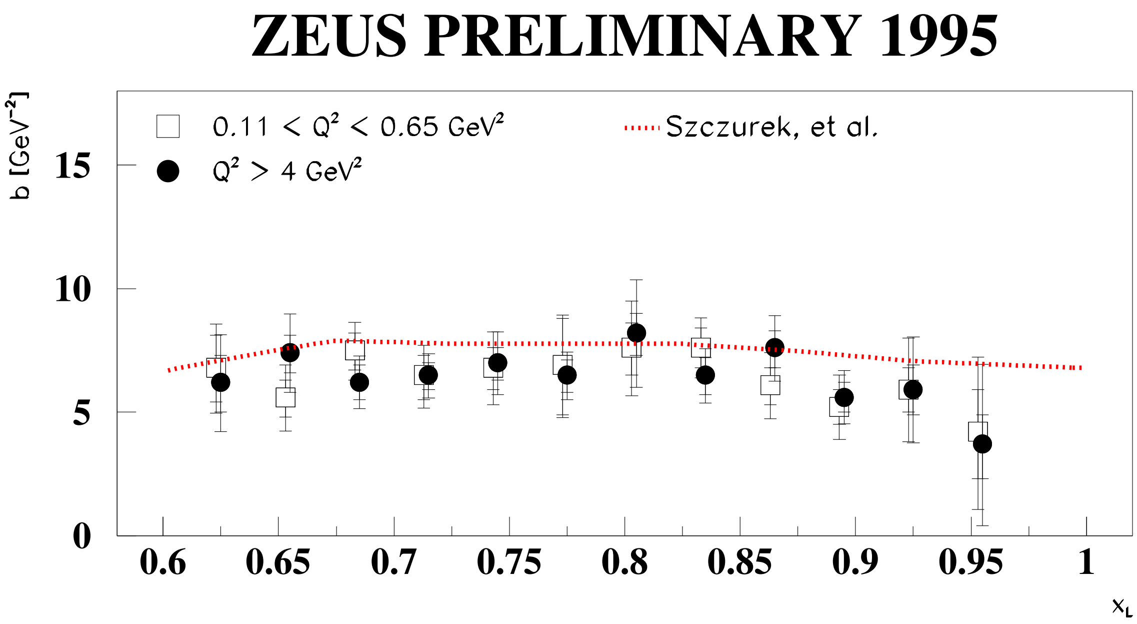

Figure 3. The measured b slopes, $dN/dp_T^2 \propto exp(-bp_T^2)$, for leading proton production in DIS ($Q^2 > 4$ GeV^2) and in the transition region ($0.1 < Q^2 < 0.8$ GeV^2) as a function of x_L. The curve shows the expectation of the model shown as a solid curve in Fig. 2.

of the produced nucleon also decreases [16, 17]. Both H1 [18] and ZEUS [19] observe a marked effect (Fig. 4). The nucleon production rate rises quickly with Q^2, but saturates in DIS where the photon becomes point-like.

5. Factorization properties

The hypothesis of limiting fragmentation [15] predicts that the lepton variables x and Q^2 completely separate from the baryon variables x_L and p_T^2. $F_2^{\rm LB}$ factorizes into a product of functions:

$$F_2^{\rm LB} = f_{lf}(x_L, p_T^2) \cdot F_{lf}(x, Q^2)$$

The observation that F_2^{LP}/F_2 is approximately constant over a large kinematic range in the leptonic variables is in good agreement with this expectation, and shows that $F_{lf} \propto F_2$. For neutrons in DIS, however, limiting fragmentation is broken at low x_L by a logarithmic rise in the neutron rate not observed at medium and high x_L.

Nucleon production by particle exchange, on the other hand, implies only a partial separation of the variables:

$$F_2^{\rm LB} = f_{ex}(x_L, p_T^2) \cdot F_{ex}(x/(1-x_L), Q^2)$$

because the energy of the exchanged particle depends on x_L. In this case, f_{ex} is a flux factor (splitting function) and F_{ex} the structure function of the exchanged particle. If F_{ex} behaves as a power law in x, as is observed for F_2 [20], then particle exchange factorization implies limiting factorization. The constancy of F_2^{LB}/F_2 in x and Q^2

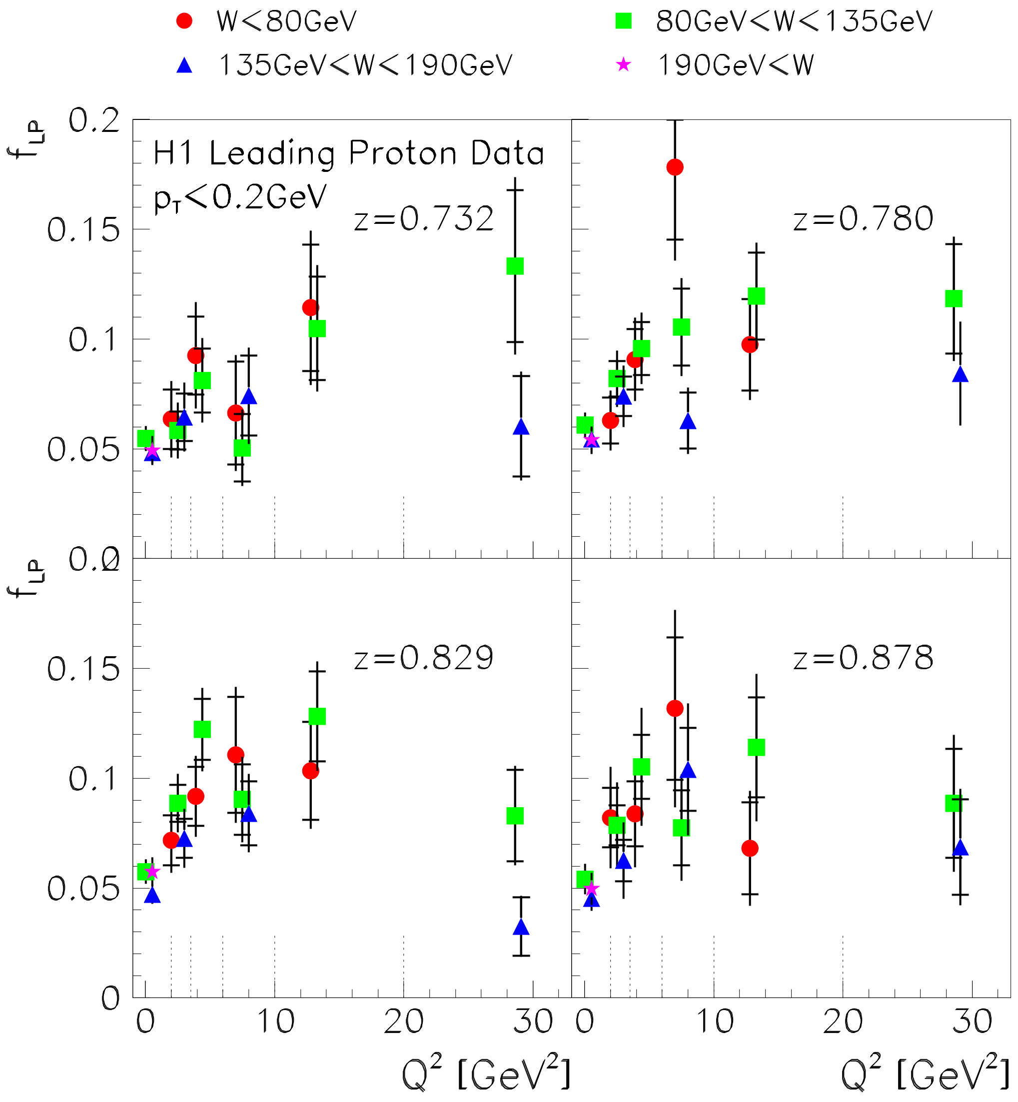

Figure 4. The ratio per unit $z \equiv x_L$, $\mathrm{f_p}$, of the number of leading proton events for four values of x_L to the total number of events in four intervals of W as a function of Q^2. The data points in the same Q^2 bin are displaced in Q^2 for visibility. The dashed lines indicate the bin limits in Q^2.

implies that F_{ex} and F_2 have a similar power law behavior in x and similar scaling violations.

6. Comparison to hadroproduction

The hadroproduction of leading nucleons has been studied in experiments at Fermilab and CERN [21–30, 32–34]. The electroproduction data at HERA are broadly similar to the hadroproduction data.

Bubble chamber data from Fermilab [22,23] show that protons produced at low p_T in hadron-hadron collisions have flat x_L spectra for $0.6 < x_L < 0.95$, exponentially falling

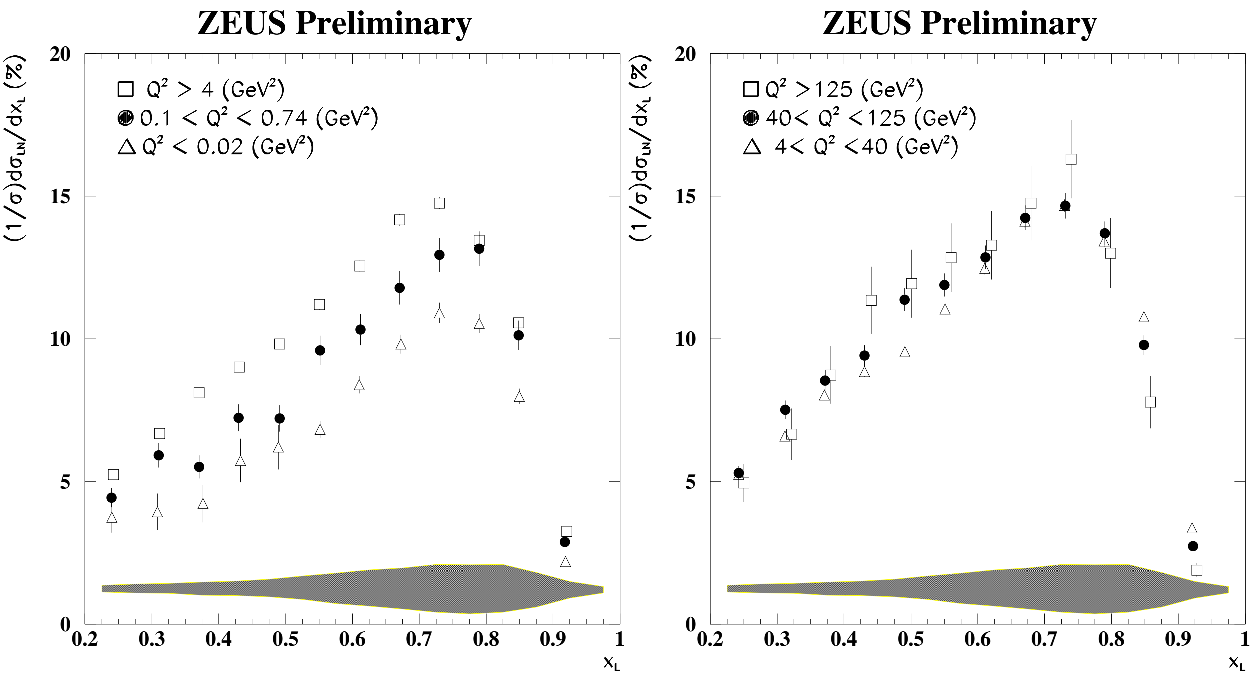

(a) (b)

Figure 5. (a) Energy spectra of neutrons in photoproduction $Q^2 < 0.02$ GeV^2, in the intermediate region $0.1 < Q^2 < 0.74$ GeV^2, and in deep inelastic scattering $Q^2 > 4$ GeV^2. (b) Energy spectrum of neutrons in DIS for three Q^2 selections: $4 < Q^2 < 40$ GeV^2, $40 < Q^2 < 125$ GeV^2, and $Q^2 > 125$ GeV^2. The points in (b) are offset for visibility. The production angle of the neutrons satisfies $\theta < 0.8$ mrad. The spectra are given as a percentage of the total ep cross section.

p_T^2 spectra, and production rates comparable to protons in DIS (!) at HERA, where the hadronic center of momentum energy is much larger ($W \approx 200$ GeV at HERA compared to 20 GeV at Fermilab). Moreover, the slopes of the p_T^2 distributions are approximately independent of x_L and have values of about 6 GeV^{-2} as in electroproduction [22].

Both the energy and angular distributions of leading neutrons at HERA are similar to hadroproduced neutrons [29–32] for $x_L \gtrsim 0.4$; however, the rate of neutrons produced in photoproduction at HERA is approximately half that expected of neutrons produced at Fermilab. The rate of protons observed in photoproduction at HERA is also half the rate expected from hadroproduction experiments at Fermilab.

7. Comparison to particle exchange models

Both H1 and ZEUS have compared the predictions of particle-exchange [2,35–37] models to their data (see Figs. 1-3). In these models the leading nucleon is produced as a result of a virtual exchange at the proton vertex. For protons, the exchanged particle can be either a meson ($f_2, \omega, \pi, \rho, a_2$) or the pomeron ($I\!P$) which contributes to diffractive scattering and carries the quantum numbers of the vacuum. Neutron production is

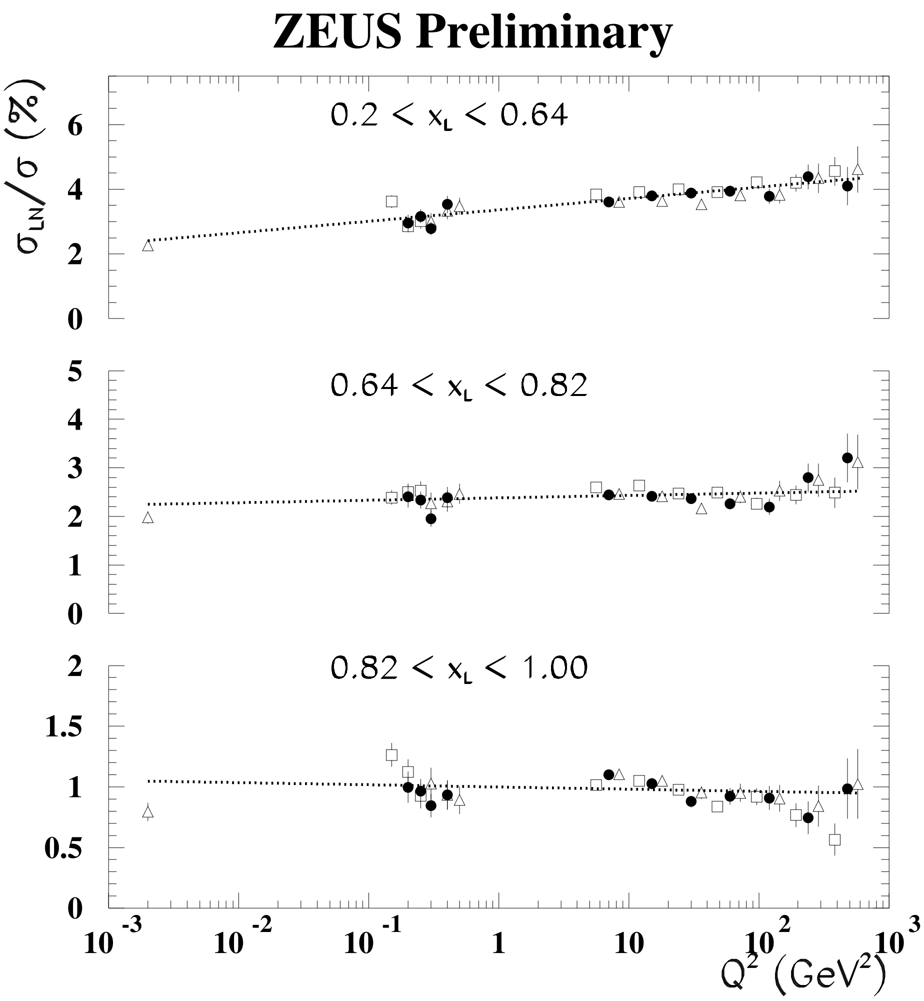

Figure 6. Neutron production as a fraction of the inclusive cross section in the photoproduction ($Q^2 < 0.02$ GeV^2), in the intermediate region ($0.1 < Q^2 < 0.74$ GeV^2), and in the deep inelastic scattering ($Q^2 > 4$ GeV^2) as a function of Q^2 in bins of y and x_L for $\theta_n \leq 0.8$ mrad. The y bins are $0.08 < y < 0.23$ (open squares), $0.23 < y < 0.37$ (solid circles), and $0.37 < y < 0.54$ (open triangles). The photoproduction point is plotted at the average value of Q^2 for the bin. The DIS points are offset for improved visibility. The dotted line shows the result of a linear fit in $\ln Q^2$, including all three y bins. The errors shown are statistical except for the photoproduction points, which have the statistical error added in quadrature with a 5% normalization uncertainty relative to the intermediate and DIS data.

simpler in that only isovector mesons (π, ρ, a_2) contribute. In these models

$$F_2^{LB(3)}(x, Q^2, x_L) = \sum_i f_{i/p}(x_L) F_2^i(x/(1-x_L), Q^2)$$

where $i = I\!P, \pi, \rho, \omega, a_2, f_2$, $f_{i/p}$ is the splitting function for $p \to B = (p, n)$ via i exchange, and F_2^i is the structure function of i. As seen in Fig. 1, the H1 x_L distributions are in good agreement with such a model. The ZEUS collaboration finds that a similar model [37] can describe both the x_L and the p_T^2 distributions of leading protons (Figs. 2,3).

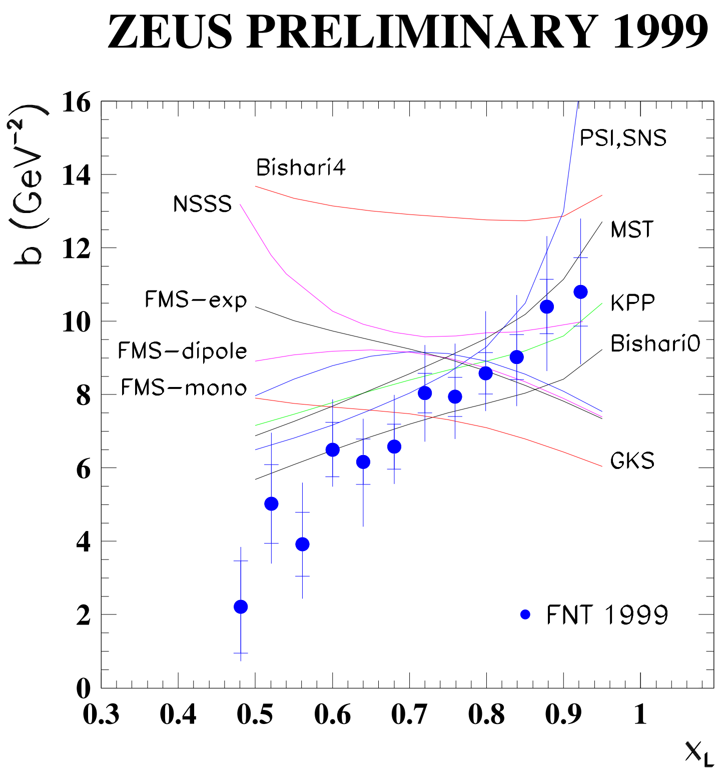

Figure 7. The measured b slopes, $dN/dp_T^2 \propto exp(-bp_T^2)$, for leading neutron production in DIS compared to various parameterizations of the pion flux factor found in the literature. See [41].

.

8. The structure of the pion

Pion exchange is expected to dominate in the production of leading neutrons [35, 36]. Hadron-hadron data from Fermilab and CERN are in agreement with this expectation [29, 31, 32]. The HERA electroproduction data present an opportunity to study pion exchange in photoproduction and DIS, to determine the $\gamma\pi$ total cross section, and to investigate the partonic structure of the pion at low x. The H1 collaboration has already published a preliminary study [2]. Here the ZEUS preliminary data [40, 41] are examined.

8.1. Effective flux method

The extraction of information on the structure of the pion is complicated by the presence of background: ρ, a_2 exchange, absorptive rescattering, off-mass-shell effects, and the indirect production of neutrons through $p \to \Delta \to n$. Fortunately, detailed knowledge of the background to pion exchange and of its decomposition into individual components is not required. Only the net effect of the background must be known. Using experimental data from the charge exchange reactions $pn \to Xp$ or $pp \to Xn$, an effective flux can be determined which implicitly accounts for the effect of the background. This avoids many theoretical uncertainties at the cost of leaving unspecified the components of the background and their relative importance to neutron production.

The effective flux of pions in the proton (effective splitting function) is determined by deconvolution ($\div$)

$$f_{eff}(x_L, t) \equiv \frac{d\sigma^{pn\to Xp}}{dx_L dt} \div \sigma^{\pi p\to X}$$

of the measured semi-inclusive differential cross section for $pn \to Xp$ and the measured πp total cross section. By construction, f_{eff} corrects for ρ and a_2 exchange, Δ production, absorptive rescattering and off-mass-shell effects.

For photoproduction the $\gamma\pi$ total cross section is obtained from

$$\sigma(\gamma\pi) = \frac{d\sigma(\gamma p \to Xn)}{f_{eff}}$$

where deconvolution is written symbolically as division. In terms of (double) ratios

$$\frac{\sigma(\gamma\pi)}{\sigma(\gamma p)} = \frac{d\sigma(\gamma p \to Xn)/\sigma(\gamma p)}{d\sigma(pp \to Xn)/\sigma(pp)} \cdot \frac{\sigma(\pi p)}{\sigma(pp)}$$

. Experiments [29, 31, 32, 34] have shown that the effective flux can be represented by

$$f_{eff}(x_L, t) = \frac{1}{4\pi}\frac{g^2}{4\pi}\frac{-t}{(t - m_\pi^2)^2}(1 - x_L)^{1-2t}$$

where m_π is the mass of the pion, t is the invariant momentum transfer in $p \to n$, and $g^2/4\pi = 29$ (this flux is labelled Bishari0 [36] in Fig. 7). f_{eff} is not expected to change significantly if the proton projectile is changed to another hadron (such as a pion) or to a real photon. The double ratio is robust for hadro- and photoproduction; however, for electroproduction, absorptive rescattering decreases as Q^2 increases. Therefore, the effective flux increases correspondingly: $f_{eff} \to f_{eff}^{\rm DIS} = 1.3 f_{eff}$ (see Fig. 5).

8.2. $\sigma(\gamma\pi)$ at high W

The leading neutron rate in photoproduction is half that expected from hadroproduction. The double ratio expression shows that $\sigma(\gamma\pi)/\sigma(\gamma p)$ is half $\sigma(\pi p)/\sigma(pp)$. Therefore $\sigma(\gamma\pi)$ is approximately one-third of $\sigma(\gamma p)$ rather than two-thirds as expected from quark counting rules. This conclusion is not changed in a more precise analysis which takes into account the difference in center of momentum energies.

8.3. F_2^π at low x

At low $Q^2 \lesssim 1$ GeV^2, F_2^π and $\sigma(\gamma^*\pi)$ are related by

$$F_2^\pi = \frac{Q^2}{4\pi^2\alpha}\sigma(\gamma^*\pi)$$

which in analogy with ρ dominance in γp interactions [20] can be written as

$$F_2^\pi = \frac{Q^2}{4\pi^2\alpha}\frac{M_0^2}{M_0^2 + Q^2}\sigma(\gamma\pi)$$

where $M_0 \approx m_\rho$, the mass of the ρ meson.

As seen in Fig. 6, ZEUS measurements show that about 2.5% of DIS events, independent of x and Q^2, have a leading neutron with $0.64 < x_L < 0.82$ and $p_T < 0.66x_L$. The constancy of this ratio with respect to x and Q^2 implies that $F_2^\pi(x, Q^2) = kF_2((1 - x_L)x, Q^2) = kF_2(0.27x, Q^2)$ with a constant of proportionality k given by

$$k = \frac{0.025}{\int\int f_{eff}^{\mathrm{DIS}}(x_L, t)dx_L dt} = 0.25$$

where the integration is over the x_L and t (p_T) range spanned by the measurement. Because $F_2(x) \propto (1/x)^\lambda$ with $\lambda \approx 0.2$ [20]

$$F_2^\pi(x, Q^2) \approx F_2(x, Q^2)/3$$

.

9. Conclusions

For leading protons the shape of the x_L spectra and angular distributions are independent of the kinematic variables x, Q^2 and x_L. Neutron production for $0.6 \lesssim x_L \lesssim 0.8$ is also approximately independent of x and Q^2, but at low and high x_L is weakly (logarithmically) dependent on them. Near the kinematic limit proton production peaks due to diffraction, while neutron production rapidly decreases to zero. The data show evidence for absorption when $Q^2 \lesssim 4$ GeV^2. Both the proton and neutron data are in good conformance with hadroproduction data from Fermilab and CERN and can be described by simple-particle exchange models. With the assumption that pion exchange dominates leading neutron production an effective flux analysis of the data shows that F_2^π has a similar x and Q^2 behavior as F_2 at low x, but only about one third its magnitude.

Acknowledgments

I thank the organizers of the workshop for a very interesting conference, and the staff of Schloss Ringberg for their hospitality. I thank my colleauges in the ZEUS Collaboration and the members of the H1 Collaboration for the opportunity to give this presentation. I thank DESY Hamburg and MPI Munich for covering the costs of the workshop.

References

[1] ZEUS Collaboration, M Derrick et al 1996 Phys. Lett. B **384** 388
[2] H1 Collaboration, C Adoff et al 1999 Eur. Phys. J. C **6** 587
[3] ZEUS Collaboration, J Breitweg et al 2001 Nucl. Phys. B **596** 3
[4] C P Burgess 2000 Phys. Rep. **330** 193
[5] V N Gribov 1999 Eur. Phys. J. C **10** 71

[6] V N Gribov 1999 Eur. Phys. J. C **10** 91

[7] C Erwez 2000 Eur. Phys. J. C **13** 503

[8] R Zoller 1992 Z. Phys. C **53** 443

[9] H Holtmann et al 1994 Phys. Lett. B **338** 363

[10] B Kopeliovich et al 1996 Z. Phys. C **73** 125

[11] A C Thomas and C Boros 1999 Eur. Phys. J. C **9** 267

[12] ZEUS Collaboration 1998 *Leading baryon production in ep scattering at HERA*, XXIX International Conference on High Energy Physics ICHEP98, Vancouver Canada, 23-29 July

[13] ZEUS Collaboration 1999 *Leading baryon production in ep scattering at HERA*, International Europhysics Conference on High Energy Physics 99 Tampere Finland, 15-21 July

[14] H1 Collaboration 2000 *Measurement of dijet cross sections with leading neutrons in photoproduction at HERA*, XXXth International Conference on High Energy Physics ICHEP2000, Osaka Japan, July 27 - August 2

[15] J Benecke et al 1969 *Phys. Rev.* **188** 2159 ; T T Chou and C N Yang 1994 Phys. Rev. D **50** 590

[16] N N Nikolaev et al 1997 *Absorptive corrections to one pion exchange and measurability of the small-x pion structure function at HERA*, *Preprint* hep-ph/9708290

[17] U D'Alesio and H J Pirner 2000 Eur. Phys. J. A **7** 109

[18] H1 Collaboration C Adloff et al 2001 *Photoproduction with a Leading Proton at HERA*, *Preprint* DESY 01-062 submitted to Nucl. Phys. B

[19] ZEUS Collaboration 2001 *Leading Baryon Production in ep Scattering at HERA*, 9th International Workshop on Deep Inelastic Scattering DIS2001, Bologna Italy, 27 April - 1 May

[20] ZEUS Collaboration, J Breitweg et al 1999 Eur. Phys. J. C **7** 609

[21] S J Barish et al 1973 *Phys. Rev. Lett.* **31** 1080

[22] J Whitmore et al 1975 Phys. Rev. D **11** 3124

[23] F C Winkelmann et al 1974 *Phys. Rev. Lett.* **32** 121

[24] F Sannes et al 1973 *Phys. Rev. Lett.* **30** 766

[25] J W Chapman et al 1974 *Phys. Rev. Lett.* **32** 257

[26] K Abe et al 1973 *Phys. Rev. Lett.* **31** 1527

[27] F T Dao et al 1973 Phys. Lett. B **45** 399

[28] J Engler et al 1975 Nucl. Phys. B **84** 70

[29] B Robinson et al 1975 *Phys. Rev. Lett.* **34** 1475

[30] W Flauger and F Mönnig 1976 Nucl. Phys. B **109** 347

[31] G Hartner 1977 *A study of pn interactions at 205 GeV/c*, Doctoral Thesis (McGill University) unpublished

[32] Y Eisenberg et al 1978 Nucl. Phys. B **135** 189

[33] V Blobel et al 1978 Nucl. Phys. B **135** 379

[34] H Abramowicz et al 1980 Nucl. Phys. B **166** 62

[35] J D Sullivan 1972 Phys. Rev. D **5** 1732

[36] M Bishari 1972 Phys. Lett. B **38** 510

[37] A Szczurek et al 1998 Phys. Lett. B **428** 383

[38] G Ingelman et al 1997 Comp. Phys. Comm. **101** 108

[39] A Edin et al 1996 Phys. Lett. B **366** 371 ; A Edin et al 1997 Z. Phys. C **75** 57

[40] ZEUS Collaboration 2000 *Energetic neutron production in e^+p collisions*, abstract 883, XXXth International Conference on High Energy Physics ICHEP2000, Osaka Japan, July 27 - August 2

[41] ZEUS Collaboration 2000 *Measurement of leading neutron p_T distributions in deep inelastic scattering at HERA*, abstract 882, XXXth International Conference on High Energy Physics ICHEP2000, Osaka Japan, July 27 - August 2